Colloids and Surfaces B: Biointerfaces 173 (2019) 539–548

Contents lists available at ScienceDirect

Colloids and Surfaces B: Biointerfaces

journal homepage: www.elsevier.com/locate/colsurfb

Folate receptor-targeted liposomal nanocomplex for effective synergistic photothermal-chemotherapy of breast cancer *in vivo*

Van Du Nguyen[a,b], Hyun-Ki Min[b], Chang-Sei Kim[a,b], Jiwon Han[b,*], Jong-Oh Park[a,b,*], Eunpyo Choi[a,b,*]

[a] School of Mechanical Engineering, Chonnam National University, 77 Yongbong-ro, Buk-gu, Gwangju, 61186, Republic of Korea
[b] Medical Microrobot Center and Robot Research Initiative, Chonnam National University, 43-26, Cheomdangwagi-ro 208-beon-gil, Buk-gu, Gwangju, 61011, Republic of Korea

ARTICLE INFO

Keywords:
Liposome
Gold nanorod
Folic acid
Drug delivery
NIR

ABSTRACT

An effective nanoparticle-based drug delivery platform holds great promise for non-invasive cancer therapy. This study explores the breast tumor regression *in vivo* by synergistic photothermal-chemotherapy based on liposomal nanocomplex (folic acid-gold nanorods-anticancer drug-liposome). The proposed liposomal nanocomplex can enhance the tumor targeting by functionalizing folic acid (FA) molecules on the surface of liposome that encapsulates both gold nanorods (AuNRs) and the doxorubicin (DOX) to combine the photothermal therapy and the chemotherapy, respectively. Herein, 7-nm gold nanorods were fabricated and co-encapsulated with DOX into nanoliposomes functionalized with FA, with an average diameter of 154 nm, for active targeting to the cancer cells. The experimental results showed that the FA targeting liposomes had better cellular uptake than the non-targeting liposomes (AuNRs-DOX-LPs). Especially, upon 5 min exposure to near infrared (NIR) irradiation (808 nm) triggered DOX release could be achieved to 46.38% in 60 min at pH 5.5. In addition, *in vitro* cell proliferation assays indicated that, with synergistic photothermal-chemotherapy, the targeting liposomes could significantly enhance the toxicity towards the cancer cells with the IC_{50} value of 1.90 ± 0.12 μg mL^{-1}. Furthermore, *in vivo* experiments on the breast tumor-bearing mice showed that the targeting liposomes could effectively inhibit the growth of the tumors using the combined strategy.

1. Introduction

Over the past 30 years, drug delivery systems using drug-loaded nanoparticles (NPs) have attracted great attentions with the aim to improve the pharmacological properties of conventional or “free” drugs. They are designed to alter the pharmacokinetics and biodistribution of the associated drugs as well as to function as the drug reservoirs [1]. With nanoscale in sizes, the NPs can passively penetrate into tumors *via* enhanced permeability and retention (EPR) effect [2]. Moreover, they can be functionalized to actively target the tumors using ligands functionalized onto the NP surfaces that allows highly specific affinity with receptors overexpressed on the targeted cells, enabling an enhanced the number of NPs up-taken to the cells by receptor-mediated endocytosis (RME) mechanism [3,4].

Currently, liposomes stand as one of the most investigated nanocarriers for delivering anticancer drugs or other therapeutic agents [5]. They are lipid vesicles that can encapsulate both hydrophobic and hydrophilic anticancer drug, and also can trigger drug release when accommodated with low phase transition lipid components [6]. In addition, it is readily to alter surfaces of liposomes with targeting ligands to allow targeted drug delivery to cancer cells. Whereas, gold nanorods (AuNRs) have unique longitudinal surface plasmon resonance peak in near infrared (NIR) window [7]. Therefore, they can efficiently converse NIR light into heat when exposed to NIR stimulus system [8]. With the above-mentioned properties, liposomes and AuNRs can be considered smart nanotherapeutics. Consequently, it is expected that the combination of these NPs into a single platform will critically enhance the therapeutic outcomes of the system in comparison with the separate uses of each individual particle.

Considered as a minimally invasive method for the treatment of solid tumors, photothermal therapy involves the conversion of NIR light absorbed to induce local heating for ablation of the cancer cells. The used of NIR light can provide soft tissue penetration of as deep as 10 cm due to minimal attenuation by hemoglobin and water [9]. In addition, with the use of NIR light, high spatial precision can be achieved without damaging normal tissues because of minimal energy absorption of the

* Corresponding authors.
E-mail addresses: judyvet@jnu.ac.kr (J. Han), jop@jnu.ac.kr (J.-O. Park), eunpyochoi@jnu.ac.kr (E. Choi).

https://doi.org/10.1016/j.colsurfb.2018.10.013
Received 24 June 2018; Received in revised form 12 September 2018; Accepted 4 October 2018
Available online 09 October 2018
0927-7765/

light by these tissues [10]. However, the main advantage of photothermal therapy is that due to the irregular distribution of the used NPs, heterogeneous heat distribution in the tumors usually occurs, complete ablation of the tumors is difficult to achieve [11]. Therefore, to improve the effectiveness of the anticancer therapy, combination of photothermal-chemotherapy strategies is proposed, by accommodating NIR laser responsive agents with anticancer therapeutics to provide a synergistic method to kill cancers with high efficacy [12–15].

Folic acid (FA) is a necessary precursor for the synthesis of nuclear acids as well as a lot of amino acids and is not produced endogenously by mammalian cells [16]. In nanoparticle drug delivery for anticancer therapy, FA is an attractive ligand for tumor targeting agent because it can bind specifically to the folate receptor (FR), which is overexpressed on tumor cells in various organs, including the breast, brain, kidney, lung, and ovary, enabling RME mechanism of NP uptake into the cells [17–19]. The high affinity between FA and FR (K_d ~ 0.1 nM) will consequently result in increased cellular uptake by FR overexpressing cancer cells, even at low FA loading on the therapeutic carriers [20]. In addition, it is reported that the FR density also seems to enhance when the stage of the cancer increases [21]. Therefore, selectively targeting to the folate overexpressing cancers can be critically improved by modifying NPs with FA moieties on their surfaces.

In this study, in combining all merits of these above mentioned materials, we develop a unique therapeutic nanosystem that enhances tumor targeting by functionalizing FA molecules on the surface of liposome that is co-loaded with both small size AuNRs and the anticancer drug (DOX) to synergistically combine photothermal therapy with chemotherapy and evaluate its therapeutic efficacy using a murine mammary carcinoma cell line (4T1), which overexpresses FRs that specifically bind with FA ligands [18,19], both *in vitro* and *in vivo* (Fig. 1). Therefore, first, we prepare and characterize the AuNRs, which are coated with bovine serum albumin (BSA). Then, we synthesize and characterize the AuNRs and DOX encapsulated liposomes with and without FA targeting moieties on the liposomal surfaces, namely FA@AuNRs-DOX-LPs (targeting liposomes) and AuNRs-DOX-LPs (non-targeting liposomes), respectively, in terms of size, shape, DOX and AuNRs encapsulation efficiency. Next, we irradiate the synthesized liposomes with NIR laser (808 nm wavelength) and study the photothermal effects and drug releasing behavior. Subsequently, we investigate the cellular uptake of the liposomes using confocal microscopy and flow cytometry. Afterwards, we evaluate the effect of the combined photothermal-chemotherapy of the liposomes against the breast cancer cells through *in vitro* cytotoxicity (MTT) assays. Finally, we use animal study to confirm the *in vivo* performance of our developed nanoplatform using 4T1 breast cancer tumor bearing mice.

2. Materials and methods

2.1. Materials

Dipalmitoyl – sn – glycerol – 3 – phosphocholine (DPPC), 1,2-distearoyl-sn-glycero-3-phosphoethanolamine-N- [methoxy (polyethylene glycol)-2000] (DSPE-PEG2000), and 1,2-distearoyl-sn-glycero-3-phosphoethanolamine-N- [folate (polyethylene glycol)-2000] (DSPE-PEG2000-Folate) were supplied by Avanti Polar Lipids Inc. (Alabaster, AL, USA). Chloroauric acid ($HAuCl_4.3H_2O$), silver nitrate ($AgNO_3$), L-ascorbic acid, sodium oleate, hydrochloric acid (HCl), sodium borohydride ($NaBH_4$), hexadecyltrimethylammonium bromide (CTAB), ammonium sulfate, HEPES, doxorubicin (DOX), cholesterol, and thiazolyl blue tetrazolium bromide (MTT) were purchased from Sigma-Aldrich (St. Louis, MO, USA). Dulbecco's modified Eagle's medium (DMEM), fetal bovine serum (FBS), antibiotics, and all other cell culture-related supplies were obtained from Gibco (Carlsbad, CA, USA). 4′,6-Diamidino-2-phenylindole dihydrochloride (DAPI) was supplied by Thermo Fisher Scientific (Waltham, MA, USA). All other solvents and reagents were of analytical grade and provided by Sigma-Aldrich.

2.2. Synthesis of AuNRs

The small size AuNRs were synthesized by a seedless technique as previously reported with minor modifications [7,22]. Briefly, 5 mL of 5 mM $HAuCl_4$, 25 mL of 0.2 M CTAB, and 25 mL of DI water were mixed

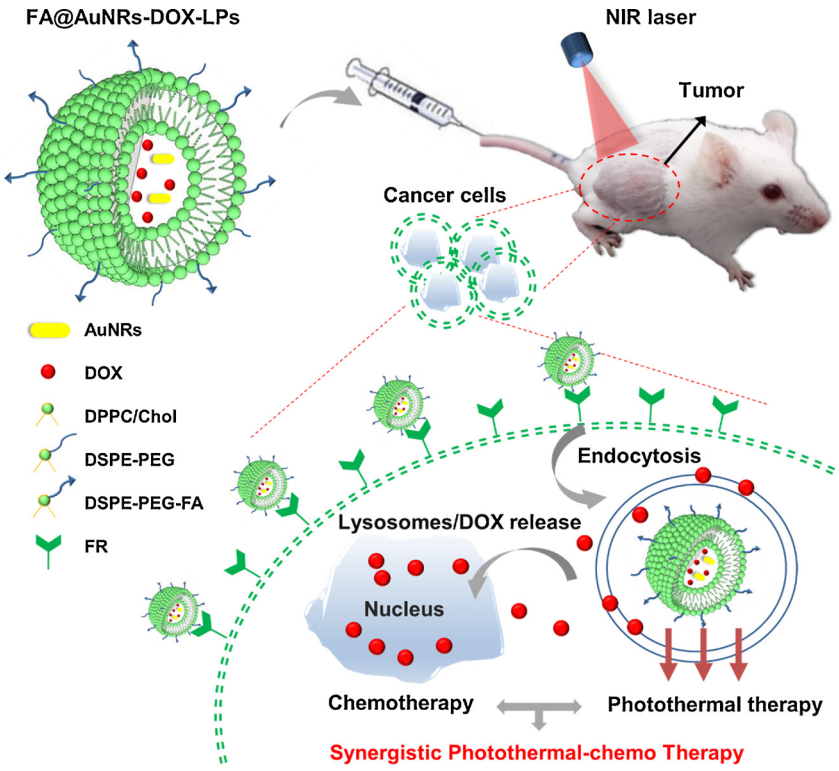

Fig. 1. Schematic diagram of synergistic photothermal-chemotherapy for breast cancer using novel folate targeting liposomes co-encapsulated with AuNRs and DOX.

in a glass flask. To the mixture, 2.5 mL of 0.1 M sodium oleate and 1.25 mL of 4 mM $AgNO_3$ were then added. After that, 40 µL of concentrated HCl (37%) were added to adjust the pH of the solution to 1–1.1, which was followed by adding 350 µL of 0.78 M ascorbic acid under gentle mixing until the solution changed from dark orange to colorless. Immediately, 75 µL of ice-cold 10 mM of $NaBH_4$ were injected with mild mixing. The solution was left in an oven at 35 °C for the reaction in 3 h. The resulting AuNRs solution was centrifuged at 17,000 rpm for 15 min to stop the reaction. After several more washes, the AuNRs precipitate was obtained and was re-dispersed in DI water. After that, the AuNRs were conjugated with bovine serum albumin (BSA). Briefly, 0.5 mL of 0.25 mM BSA in PBS (pH 7.4) was added to 5 mL of the AuNRs solution, followed by vigorous stirring overnight at room temperature. Then, the reaction was terminated using centrifugation at 6000 rpm for 5 min and the excess BSA in the supernatant was removed. Finally, the resulting AuNRs precipitate was re-suspended DI water and stored at 4 °C for further use.

2.3. Preparation of liposomes

Non-targeting (AuNRs-DOX-LPs) and targeting (FA@ AuNRs-DOX-LPs) liposomes were prepared using a thin-film hydration as previously reported [23]. In brief, DPPC: Chol: DSPE-PEG2000 (non-targeting) or DPPC: Chol: DSPE-PEG2000: DSPE-PEG2000-Folate (targeting) with the molar ratio of 80:20:5 and 80:20:4.5:0.5, respectively, were dissolved in chloroform/methanol solution (9/1, v/v) in a 50-mL pear-shaped flask. The solvents were evaporated under vacuum to form a thin film using a rotary evaporator (Büchi R-300, Flawil, Switzerland). The flask was then left in vacuum condition overnight to completely remove any track of the solvents. Multiple lamellar vesicles (MLVs) were obtained after hydrating the thin film with 2 mL of 250 mM ammonium sulfate solution containing AuNRs at 50 °C in a water bath for 30 min [23]. Next, the MLVs were downsized by sonication and then passed through 200 nm polycarbonate membranes (11 times) using a mini extruder (Avanti Polar Lipids). Subsequently, the preparation was subjected to gel filtration on Sephadex G25 equilibrated with PBS. DOX was actively loaded into the liposomes using ammonium sulfate gradient. Briefly, DOX.HCl (2 mg mL^{-1}) were incubated with the liposomal suspension in a water bath at 35 °C for 2 h. The unloaded DOX were separated using gel filtration as aforementioned. While free AuNRs were removed by centrifugation as previously described [7]. Finally, the obtained liposomes were stored at 4 °C for further use.

2.4. Characterization of AuNRs and liposomes

2.4.1. Size distribution and zeta potential

The size of the liposomes and the zeta potential of the AuNRs were analyzed using a Zeta-PSA platform (ELS-8000, Otsuka Electronics, Osaka, Japan). Before the measurement, the AuNRs and the liposomes were diluted with PBS. Each formulation was investigated in triple measurement with independent samples. For the liposomes, experiments were performed with and without FA coating on the liposomal surfaces.

2.4.2. Transmission electron microscopy (TEM)

The morphologies of AuNRs and liposomes and the encapsulation of AuNRs into the liposomes were investigated using TEM (TECNAI F20 ST, FEI Company, Hillsboro, OR, USA). Briefly, 10 µL of the diluted sample were prepared onto a carbon-coated grid, dried at room temperature, and investigated under the TEM system.

2.4.3. X-ray Electron Spectroscopy (XPS)

Surface chemistry of prepared liposomal formulations with and without folate ligand was investigated using XPS (ESCA-2000 Multilab apparatus, VG Microtech, London, UK) to analyze the chemical compositions on the surfaces of the liposomes with the binding energy ranged from 0 to 1000 eV to determine carbon, nitrogen, and oxygen contents.

2.4.4. Determination of encapsulation efficiency (EE)

The DOX content entrapped in the liposomes was determined by measuring the fluorescent intensity of the liposomal suspension after disrupting the liposomes with a 1% Triton X-100 to obtain liposomal lysate at the excitation/emission wavelength of 485/590 nm using a multimode plate reader (Varioskan Flash, Thermo Scientific, Waltham, CA). The AuNRs concentrations in the liposomes were measured from the Au amount obtained by an inductively coupled plasma-atomic emission spectrometer (ICP-OES, Optima 4300DV, PerkinElmer, Wellesley, MA) in the lysate of the liposomal solution. In all experiments, the EE (%) was calculated by comparing the encapsulated amount with the initially added.

2.5. Photothermal effect using NIR laser

The photothermal effects of the liposomes with different Au concentrations were evaluated using NIR equipment at an irradiation wavelength of 808 nm. Briefly, 1 mL of aqueous suspensions of the samples were prepared in cuvettes and then exposed to the NIR laser light for 5 min (808 nm, power of 1.5 W). Temperature changes in each cuvette throughout the experiment were recorded using a FLIR thermal imaging camera (E64501, FLIR Systems, Wilsonville, OR, USA) to get a video file, from which temperature change profiles of the samples were generated.

2.6. In vitro drug release

To study the release behavior of DOX from the liposomes, samples containing 0.5 mL of the liposomal suspensions in PBS (pH 5.5 and 7.4) at a concentration equivalent to 5 µg/mL free DOX were incubated in 1.5-mL tubes at 37 °C in a water bath for 60 min. For the NIR irradiation samples, the tubes exposed to the NIR laser for 5 min from the beginning of the experiments. After that, the tubes were immediately placed back into the water bath and the experiments continued. Cumulative DOX release from the liposomes was calculated using following equation:

$$Cumulative\ release\ (\%) = \frac{f_t - f_0}{f_{100} - f_0} \times 100$$

where f_t is the fluorescence at time point t, f_0 is the initial fluorescence of the liposomal suspension at the beginning of the incubation time, and f_{100} is the fluorescence of Triton X-100 prepared samples [24].

2.7. Uptake studies

2.7.1. Cell culture

Mouse breast cancer cells (4T1) and mouse origin fibroblast cells (NIH3T3) cells were purchased from the American Type Culture Collection (Manassas, VA, USA). The cells were maintained in DMEM supplemented with 10% FBS and 1% antibiotic solution and were kept in a humidified incubator at 37 °C in 5% CO_2.

2.7.2. Confocal laser scanning microscopy (CLSM)

Cellular uptake of the free DOX and DOX-loaded liposomes (FA@AuNRs-DOX-LPs and AuNRs-DOX-LPs) was investigated using CLSM (TCS SP5/AOBS/Tandem, Leica, Wetzlar, Germany). Briefly, 4T1 cells were plated on ∅18-mm coverslips accommodated in a 12-well plate, which were previously sterilized at 120 °C and completely dried in an oven at 80 °C and prepared at a density of 1.5×10^5 cells/well overnight to allow cell attachment. Then, the used media were discarded, and the cells were treated with either AuNRs-DOX-LPs, FA@AuNRs-DOX-LPs, or FA@AuNRs-DOX-LPs + NIR irradiation in

DMEM at 37 °C and 5% CO_2. For the NIR treatment group, after 2 h of incubation, the cells were rinsed several times with PBS and exposed to the NIR laser for 5 min. For the negative control group, the cells were treated with only fresh media. In addition, for competitive inhibition study, the cells in one group were treated with free folic acid (1 mM) at 2 h prior to the experiments [25]. Upon completion, the supernatants were discarded, and the cells were rinsed three times with cold PBS. Subsequently, the cells were fixed with 4% paraformaldehyde (PFA) for 10 min. Then, the cells were washed two times with cold PBS and the nuclei were stained with DAPI (1 μg mL^{-1}) for 10 min. Finally, the cells were rinsed three times with PBS and imaged using CLSM [6].

2.7.3. Quantitative flow cytometry analysis of cellular uptake

Quantitative cellular uptake of the liposomes was determined using flow cytometry (FACS) [26]. In brief, 4T1 cells were inoculated overnight in a 6-well plate (5×10^5 cells mL^{-1}). Next, the cells were treated with samples as previously indicated. Afterwards, the cells were washed, harvested, fixed with 4% PFA, and re-suspended in 0.5 mL of PBS. At least 1×10^4 cells in the suspension was analyzed with a MACSQuant VYB flow cytometer (MACS Miltenyl Biotec, Auburn, CA, USA).

2.8. In vitro cytotoxicity

The cytotoxicity of the liposomes against the cancer cells was investigated by MTT assay [6]. Briefly, 1×10^4 4T1 cells were plated in DMEM in a 96-well plate (SPL Life Sciences). The cells were incubated in an incubator (37 °C and 5% CO_2) for 24 h. Next, the media were discarded, and the cells were treated with various doses of free DOX, AuNRs-DOX-LPs, FA@AuNRs-LPs, or FA@AuNRs-DOX-LPs prepared in DMEM media. For the photothermal treatment groups, namely FA@AuNRs -LPs + NIR and FA@AuNRs-DOX-LPs + NIR, the cells were exposed to the NIR laser for 5 min after a 2 h incubation with the targeting liposomes. After 24 h, the media in the wells were aspirated and the cells were rinsed with PBS. Next, the cells were prepared with MTT in DMEM (0.5 mg mL^{-1}) and incubated for a further 3.5 h. Subsequently, the medium in each well was replaced with 100 μL of DMSO. The viability of the cells was measured using an ELISA plate reader (Varioskan Flash, Thermo Scientific, Waltham, CA) at 570 nm. IC_{50} values, the inhibitory concentration, were calculated using regression of the experimental data. Additionally, the cytotoxicity of the free-drug AuNRs-LPs and FA@AuNRs-LPs against NIH3T3 and 4T1 cells was evaluated as aforementioned with predetermined concentrations of liposomes added to the cells. Finally, in all experiments, the viabilities of the cells were calculated by the below equation:

$$Viability\ of\ cells\ (\%) = \frac{Absorbance_{\ Sample}}{Absorbance_{\ Control}} \times 100$$

To visualize the live/dead cells after the treatment, we adopted calcein AM/ethidium homodimer-1 (EthD-1) co-stained assay (Thermo Fisher Scientific). In brief, 2×10^4 4T1 cells per well were seeded and treated with PBS, free DOX, FA@AuNRs-DOX-LPs, or FA@AuNRs-DOX-LPs + NIR. The laser (808 nm, 1.5 W) was employed at 2 h in 5 min. Then, the cells were co-stained with calcein AM (2 μM) and EthD-1 (4 μM) following the manufacturer's protocol. Finally, the cells were rinsed with PBS and observed under the CLSM [27].

2.9. In vivo study

2.9.1. Animal models

Balb/c mice were obtained from Orient Bio Inc. (Seoul, Korea) and were handled in accordance with the guidelines of the Animal Care and Use Committee of Chonnam National University, Korea. To induce a solid breast tumor, 4T1 cells (1×10^6) suspended in 100 μL of PBS were subcutaneously injected into the right flank of each mouse. After approximately 10 days, when the 4T1 tumors were formed and reached about 100 mm^3, the mice were randomly divided into six groups (n = 5 per group) and intravenously injected with either PBS, free DOX, AuNRs-DOX-LPs, FA@AuNRs-DOX-LPs, FA@AuNRs-LPs + NIR, or FA@AuNRs-DOX-LPs + NIR (DO X 2.5 mg/kg) *via* tail vein. For NIR treatment groups, 48 h after tail vein injections with samples, the tumors were exposed to the NIR laser with the power of 1.5 W, in 5 min. Tumor sizes were monitored and measured using a digital caliper in every 2 or 3 days for 2 weeks. The tumor volume was determined using the following formula: $L \times W^2/2$. Where L and W denote the longest and shortest dimensions of the tumor, respectively [28].

2.9.2. Thermal imaging

Mice bearing 4T1 tumors treated with either PBS, or FA@AuNRs-LPs, or FA@AuNRs-DOX-LPs were irradiated with the 808 nm for 5 min and the temperature changes were observed using the FLIR thermal imaging camera.

2.9.3. H&E examination

For H&E examination, the 4T1 tumor-bearing mice were treated FA@AuNRs-DOX-LPs. The mice were scarified at the end of the observation period. The main organs were harvested and embedded in optimal cutting temperature (OCT) compound, followed by storage at −80 °C before use. The organ tissue sections (10 μm) were mounted onto slides and then fixed with pre-cooled methanol (80%) for 5 min and washed two times with PBS. The sections were then stained with H &E following the standard protocol and examined under an optical microscopy [29].

2.10. Statistics

Data were shown as means with standard deviations of the three samples. The comparison of data was performed using the Student's *t*-test (* represents $P < 0.05$; ** represents $P < 0.01$).

3. Results

3.1. Preparation and characterization of AuNRs and liposomes

The AuNRs were synthesized using seedless method, in which nucleation and growth appear in the same solution. The use of this method will produce the AuNRs with smaller sizes in comparison with seed-mediated two-step methods, thereby resulting in easier cellular uptake and encapsulation into the liposomal carriers. As the results, Fig. 2a shows the TEM image of the prepared AuNRs with high yield of nanorods and few byproducts. The AuNRs had typical dimensions of 29 nm × 7 nm (aspect ratio of 4.1) as calculated from TEM images using ImageJ software (NIH). Figure S1 displays the absorbance spectrum of the nanorods in the UV–vis-NIR window of 400–1000 nm, having the longitudinal surface plasma resonance peak at 798 nm. To reduce the toxicity of the AuNRs caused by CTAB as an emulsifier, BSA was coated to the nanorods *via* electrostatic interaction. By measuring the zeta potentials of the AuNRs, it is shown that the zeta potentials changed from highly positive (33.50 ± 1.15 mV) to negative values (-9.48 ± 0.34 mV) before and after coating with BSA, respectively, thus verifying the successful BSA coating on the nanorods' surfaces.

The anticancer drug (DOX.HCl) and fabricated AuNRs were co-incorporated into the aqueous cores of the liposomes. To evaluate the enhanced cellular uptake ability of the targeting liposomes, we prepared two kinds of vesicles, namely FA@AuNRs-DOX-LPs and AuNRs-DOX-LPs. Typically, TEM images showed that the liposomes had smooth spherical surfaces without any critical cracks and holes (Fig. 2b). It is also indicated that the AuNRs were successfully encapsulated the liposomes ((Fig. 2b-Inset). The engulfment of the nanorods into the liposome was further confirmed by energy-dispersive X-ray Spectroscopic (EDS) pattern of the liposome, which shows the Au components in the liposomes (Figure S2). In addition, both liposomes

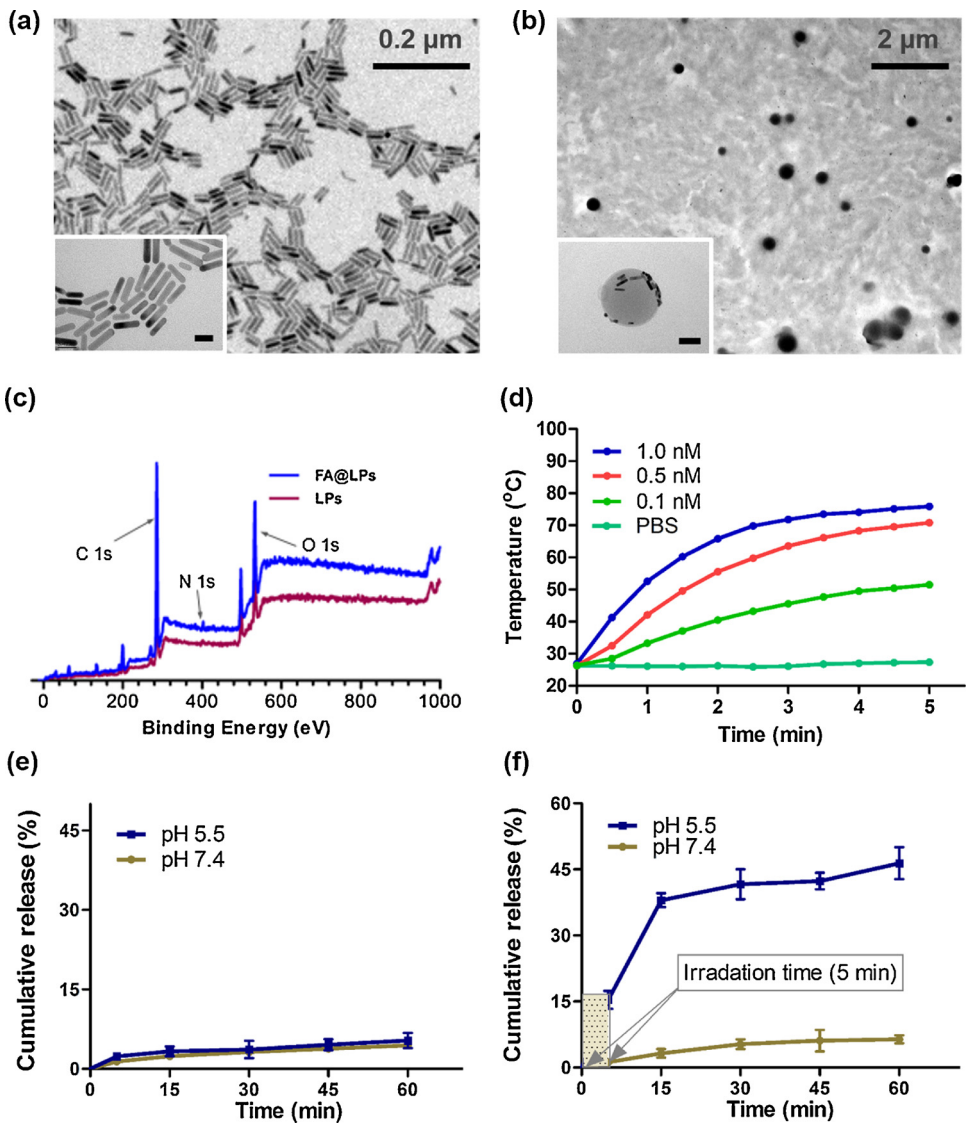

Fig. 2. Characterizations of proposed targeting liposomes: (a) Transmission electron microscope (TEM) images of AuNRs at low magnification and high magnification (inset, scale bar: 20 nm). (b) TEM images of the targeting liposomes (FA@AuNRs-DOX-LPs) at low magnification, and (inset, scale bar: 50 nm) that of a single targeting liposome at high magnification showing the successful encapsulation of AuNRs inside. (c) X-ray photoelectron spectroscopy patterns of the targeting and nontargeting liposomes without AuNRs and DOX. (d) Temperature change profiles of liposomes with different AuNRs concentrations under 808 nm NIR light irradiation. (e) and (f) drug release profiles of the liposomes without and with NIR (808 nm) irradiation in 5 min, respectively, bars represent S.D. (n = 3).

had a narrow size distribution ranging from 100 to 200 nm. However, the FA@AuNRs-DOX-LPs had a slightly higher in average size of 154.32 ± 1.15 nm, compared to 142.05 ± 2.81 nm of AuNRs-DOX-LPs (Figure S3). The results might be contributed to the addition of the FA coating onto the surfaces of the targeting liposomes. Fluorescent intensity measurement results revealed that the DOX EE of the non-targeting and targeting liposomes were about 56.11 ± 3.55% and 54.73 ± 2.13%, respectively. Inductively coupled plasma-atomic emission spectrometer (ICP-OES) showed that 30.25 ± 1.56% and 25.12 ± 3.15% of AuNRs were successfully loaded inside the two liposomes, respectively (Table S1), which could be attributed to the fact that the prepared AuNRs were well dispersed into the hydration solution. The results were in line with the previously published in literature where AuNRs could be loaded into nanocarriers with very high efficiency [10].

To further confirm the incorporation of FA ligands on the targeting liposomes, we prepared the nontargeting and targeting liposomes without encapsulation of DOX and AuNRs. The powder of the lyophilized liposomes was prepared in an X-ray electron spectroscopy (XPS) device. And the C, N, O elements of the non-targeting and targeting liposomes were scanned and illustrated in Fig. 2c. As the results, it was found that in both types of liposomes, XPS scan detected N1s signal at 398 eV; while peaks at 285 eV and 532 eV are corresponding to C1s and O1s, respectively. In addition, a narrow scan of the N1s binding energy region uncovered an intense peak (398 eV), which was attributable to the N atoms on the surfaces of the targeting liposomes. This intense signal was due to the additional N element of the folate presenting onto the outer surface of the targeting liposomes [4], thereby confirming that the functionalization of the FA ligands for the active targeting purpose was successfully achieved. In addition, TEM images and size distribution of the prepared liposomes without the encapsulation of DOX and AuNRs also verified the inclusion of FA onto the targeting liposomal surfaces (Figure S4 and Figure S5).

The photothermal conversion ability of FA@AuNRs-DOX-LPs with different concentrations for 5 min are shown in Fig. 2d and Figure S6. Upon exposure to NIR irradiation, the temperatures of the liposomal solution increased to approximately 75.9 °C (1 nM); meanwhile that of the PBS solution only fluctuated around room temperature of about 27.3 °C. The results indicate that the nanorod component in the liposomal suspension could effectively and rapidly convert NIR light into thermal energy, which is necessary to obtain local hyperthermia and triggered drug (DOX) release from the liposomes using an external NIR device.

The drug release characteristics of the FA@AuNRs-DOX-LPs were studied as described above based on the fact that DOX shows the self-quenching characteristics within the liposomes and fluorescent intensity increases when the drug was released into the surrounding medium [24]. In addition, we performed experiments with the

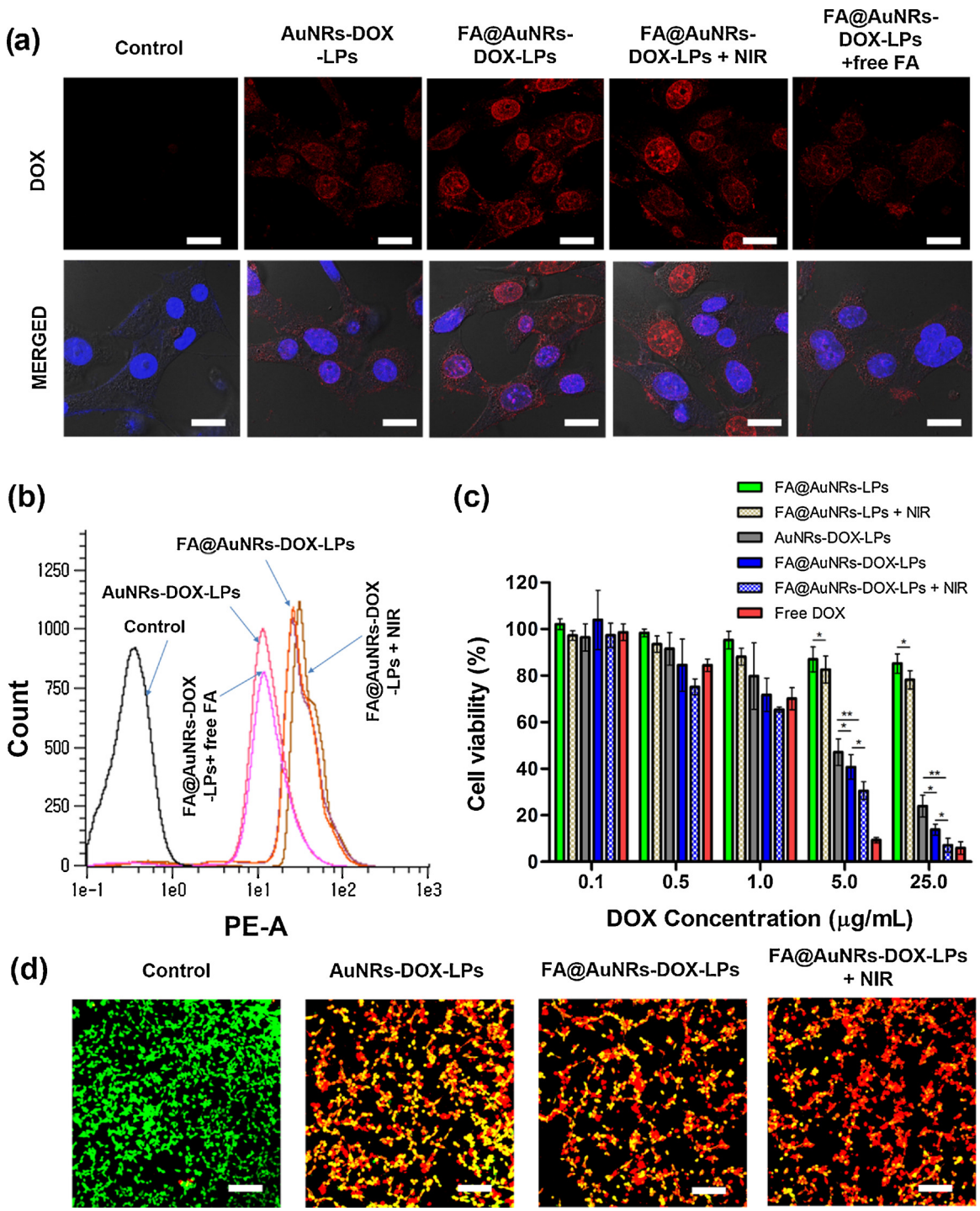

Fig. 3. *In vitro* evaluation of synergistic effect of photothermal-chemotherapy on 4T1 cells using targeting liposomes: (a) *In vitro* cellular uptake analysis of different liposomal samples into 4T1 breast cancer cells using CLSM images: Blue signal is from DAPI and red signal is from DOX (Scale bars: 20 μm). (b) Quantitative cellular uptake using FACS. And (c) *In vitro* cytotoxicity test of different samples against 4T1 cells at various DOX concentrations after 24 h incubation, $^{**}P < 0.01$ and $^{*}P < 0.05$, bars represent S.D (n = 3). (d) CLSM images of calcein AM/EthD-1 stained 4T1 cells treated with PBS, non-targeting, targeting liposomes, and targeting liposomes with NIR irradiation; green indicates the live cells and red indicates the dead cells (Scale bars: 100 μm) (For interpretation of the references to colour in this figure legend, the reader is referred to the web version of this article).

targeting liposomes and NIR laser irradiation (Fig. 2c-d). For both cases, we studied the drug release behaviors in two pH environments, *i.e.* pH 7.4 and 5.5. As the results, without NIR irradiation, the liposomes showed very low DOX release rate (less than 5%) in both pH values (Fig. 2e). With NIR irradiation, same release pattern and rate were also observed when the pH value of the solution was 7.4; however, with the pH value of 5.5, critical drug amount (46.38%) was liberated from the liposomes (Fig. 2f). These results confirmed that NIR laser irradiation could be used to trigger drug release from the liposomes with the pH value similar to that of the endosomal environments, suggesting an approach for enabling on-demand drug release only to the target tissues to avoid damaging nontargeted tissues [11,28].

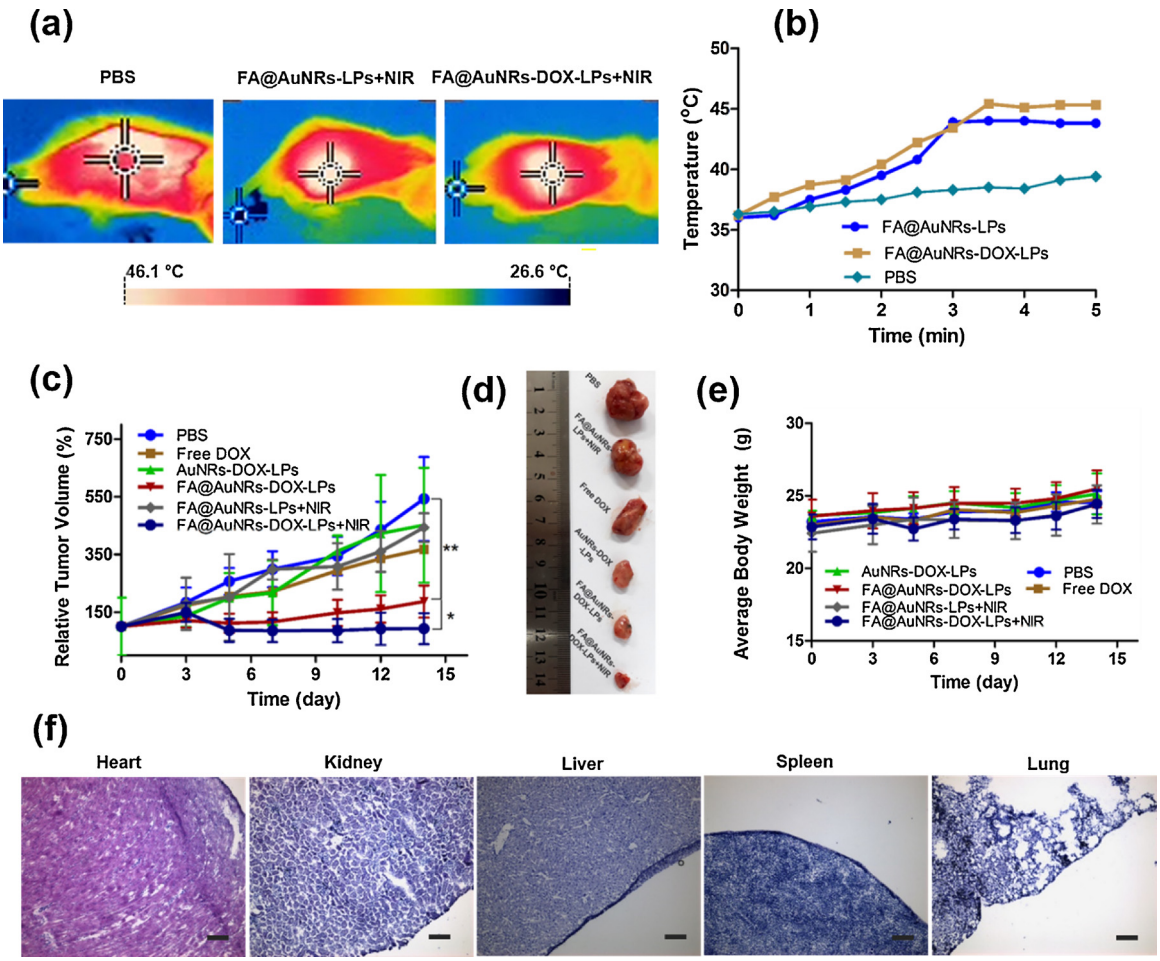

Fig. 4. *In vivo* evaluation of synergistic effect of photothermal-chemotherapy on 4T1 tumor-bearing mice using targeting liposomes: (a) and (b) photothermal graphs and temperature change profiles, respectively, of mice treated with PBS, targeting liposomes without DOX (FA@AuNRs-LPs), or targeting liposomes with DOX (FA@AuNRs-DOX-LPs). (c) Tumor growth profiles of mice after injections of samples; tumor volumes were normalized to their initial sizes, $^{**}P < 0.01$ (compared with PBS) and $^{*}P < 0.05$ (compared with FA@AuNRs-DOX-LPs w/o NIR irradiation), bars represent S.D (n = 5). (d) Typical excised tumor sections of mice treated with different samples. (e) Body weight profiles of tumor-bearing mice in 14 days after injection of samples, bars represent S.D (n = 5). (f) H&E staining images of sliced sections of major organs of the mice treated with FA@AuNRs-DOX-LPs (Scale bars: 50 μm).

3.2. In vitro cell study

Cellular uptake was investigated using CLSM. DAPI was used to stain the cellular nuclei to separate with the red signal from DOX. In the experiments, AuNRs-DOX-LPs and FA@AuNRs-DOX-LPs were added to the 4T1 cells. For the targeting liposomes with NIR laser treatment group, cells were irradiated for 5 min after a 2-h incubation. Cellular uptake findings are shown in Fig. 3a. It was found that a significantly stronger signal was recorded in the group of the FA@AuNRs-DOX-LPs LPs treatment group compared to the non-targeting group. These results could be attributable to the FA molecules on the targeting liposomes which specifically bound to the FRs overexpressed on the 4T1 cells, enabling RME uptake pathway. Therefore, the internalization of the targeting liposomes into the cells would be due to both pathways, passive endocytosis and RME. However, AuNRs-DOX-LPs could only enter the cells by passive targeting, thereby reducing the DOX fluorescent signal in the cells. In the NIR treatment group, the signal was higher than that in the NIR untreated group, suggesting that NIR irradiation could enhance the cellular uptake of the liposomes. The result may be attributed to the membrane permeability of the cells upon laser irradiation as previously reported [28]. In addition, DOX signals were highly detected in the nuclei of the cells from the NIR treatment group, suggesting that DOX was released from the liposomes following NIR irradiation and entered the nuclei. Similar results were also obtained with the quantitative analysis using the FACS (Fig. 3b). The liposomes with FA targeting ligands, with or without NIR irradiation, had much higher cellular uptake rates than the liposomes without FA. Additionally, in the competitive inhibition study, due to the addition of free FA, the FRs overexpressed on the surfaces of the cells were blocked and the interactions between the FA molecules of the targeting liposomes and the receptors were inhibited, therefore the RME pathway to the cells of the liposomes was prevented, leading to the reduced DOX signal from this group [11]. These findings confirmed the role of FA in enhancing uptake through active targeting *via* RME. In addition, the NIR laser exerted a meaningful effect on cellular uptake of the targeting liposomes.

MTT assays were performed to evaluate the cytotoxicity of the blank AuNRs-LPs and FA@AuNRs -LPs against NIH3T3 and 4T1 cells. As depicted in Figure S7, when the liposomal concentration increased to 1 mg mL^{-1}, no significant cell death was observed in either cell line. These results imply that the prepared liposomes exerted no specific cytotoxicity on either normal or cancer cells, suggesting that the liposomes were biocompatible and could be used for *in vivo* applications.

Next, the therapeutic efficacy of the prepared DOX loaded liposomes was evaluated using 4T1 cells, which are known to overexpress FRs [18,19]. As shown in Fig. 3c, cell viabilities following liposomal treatment were dose-dependent. Free-drug targeting liposomes with NIR irradiation exerted meaningful cell cytotoxicity. While the

FA@AuNRs-DOX-LPs induced significantly higher toxicity than the AuNRs-DOX-LPs. The results could be explained by the higher cellular uptake following specific binding of FA from the liposomal surfaces of the targeting liposomes to FRs, thereby releasing higher amounts of the drug inside the cells. The IC_{50} values AuNRs-DOX-LPs and FA@AuNRs-DOX-LPs were 4.92 ± 0.57 μg mL^{-1} and 3.15 ± 0.26 μg mL^{-1}, respectively (Table S2). A remarkable finding was that with the addition of NIR irradiation, cell viability drastically reduced. The IC_{50} value for the irradiation targeting group was 1.90 ± 0.12 μg mL^{-1}, which was quite close with the value of free DOX (1.71 ± 0.30 μg mL^{-1}) (Table S2). This result could be attributable to the local hyperthermia and the triggered drug release from the liposomes upon NIR irradiation, leading to the combined killing effects towards the cancer cells.

In addition, calcein AM/EthD-1 co-staining assay was performed to intuitively evaluate the efficiency of the cancer cell treated with PBS, AuNRs-DOX-LPs, FA@AuNRs-DOX-LPs, or FA@AuNRs-DOX-LPs + NIR (Fig. 3d). Green and red signals indicate live and dead cells, respectively. It was obvious to note that the formulation FA@AuNRs-DOX-LPs + NIR with the synergistic therapy showed the best antitumor effects on 4T1 cells. The results were analogous with those in the cellular uptake and MTT assays, and also were in line with the results reported recently in literature [27].

3.3. *In vivo* evaluation on breast tumor bearing mice

Based on the excellent *in vitro* performance of the developed nanoplatform, we further evaluated the performance *in vivo* using 4T1 tumor bearing mice. First, 1×10^6 cancer cells were subcutaneously injected to the right flank of each mouse, and the tumors with the volumes around 100 mm^3 were formed in approximately 10 days. Fig. 4a and Fig. 4b represent the typical thermal photographs and thermal changing profiles of the mice treated with either PBS, or FA@AuNRs-LPs, or FA@AuNRs-DOX-LPs. Under NIR laser irradiation, the temperature of the tumors injected with PBS (control) could slightly increase to around 39 °C, whereas those of the tumors treated with the liposomal therapeutics could rapidly approach to more than 43 °C for both type of samples, which is sufficient for tumor ablation [28,30]. The *in vivo* anti-cancer therapeutic efficacy the prepared liposomes were evaluated by examination of the tumor growth. In this experiment, the tumor size of each mouse was normalized to its initial size and was indicated as relative tumor growth in volume (%). As shown in Fig. 4c and Fig. 4d, mice treated with all samples showed significant delay in tumor growth in comparison with the control group (PBS treated); even when the mice treated with FA@AuNRs-LPs + NIR (with no DOX), indicating the ability of killing cancer cells of the AuNRs encapsulated liposomes using photothermal therapy. It is worth mentioning that the group treated with FA targeting liposomes (FA@AuNRs-DOX-LPs) displayed significant suppression on tumor growth compared to the group treated with non-targeting liposomes (AuNRs-DOX-LPs). The results could be attributed to the role of FA ligands that bound specifically to FA receptors expressed on 4T1 tumor cells, as indicated in many current studies [31], thereby enhancing the cellular uptake of the targeting liposomes, to the cancer cells *via* RME pathway after the liposomes had penetrated into tumor utilizing EPR effect. An important finding was that when the group treated with targeting liposomes and irradiated with NIR laser in 5 min, the tumor growth was significantly regressed compared to the initial tumor. Fig. 4e shows the body weight profiles of tumor-bearing mice in 14 days after injection of samples, indicating no significant systemic toxicity of the injected samples to the mice during the examined time [32]. In addition, H&E examinations of the major organs, including heart, kidney, liver, spleen, lung, from the mice treated with the targeting liposomes showed no severe toxicity, thus further confirming the safety of the developed formulation (Fig. 4f). After all, the experimental results confirmed the initial scenario about the synergistic effects of photothermal chemotherapy with the targeting liposomes to effectively regress the tumor growth.

4. Discussion

In cancer treatment, it is well known that the photothermal monotherapy induces heterogeneous distribution of heat, resulting in insufficient tumor damage especially at the boundary of the tumor tissues [32]. Meanwhile, chemotherapy suffers from serious adverse side effects and drug resistance [33]. Therefore, the combination is considered as a potentially promising strategy for the treatment of cancers [11]. In our recently published works, we have prepared and proved *in vitro* the feasibility of using various ligands conjugated NPs, namely hybrid HA-conjugated nanoliposomes and nanostructured lipids carriers, and FA-conjugated polydopamine nanoparticles, to tackle the breast cancers [11,31,34]. In these NP systems, the conjugations of the targeting ligands were shown to significantly increase cellular uptake of the NPs to cancer cells. In addition, it was proven that the encapsulation of NIR light sensitive agents into the NPs could markedly trigger the drug liberation from the carriers.

Furthermore, lately, there are numbers of studies on FR targeting utilizing multicomponent liposomes composing of FA-conjugated lipids [24,35]. In these works, the liposomes were co-encapsulated with DOX and superparamagnetic nanoparticles (SPIONs). The functionalization of the FA ligand was shown to critically enhance the cellular uptake of the targeting liposomes in various cell lines, including human cervical cancer cells (HeLa) and/or KB cells, in comparison with their non-targeting counterparts. With the encapsulation of SPIONs into the liposomes, the release of DOX was controlled with the application of alternative magnetic fields. Although, the studies pioneered the field and showed encouraging results, only *in vitro* evaluation was conducted to assess the therapeutic performance of these NP-platforms. Therefore, in this study, we have designed and performed *in vitro* characterization and *in vivo* evaluation of a unique FA-targeting multifunctional liposomal system on a mouse origin breast cancer cell line. With the emerging application of an alternative external stimulating system (NIR-based system), the use of small size AuNRs may offer more advantages in thermal conversion ability than that of the SPIONs since they possess typical LSPR peak in the NIR window [7,36].

The synthesized liposomes were functionalized with FA to enable active targeting to cancer cells, thereby enhancing the cellular uptake of the liposomes. The functionalization of the FA ligands was confirmed by the changes in size as well as XPS patterns in comparison with the non-targeting liposomes. The average sizes of the liposomes were adjusted to be around 150 nm, allowing the passive penetration of the systems *via* EPR effect in combination with active targeting using FA ligand *via* receptor mediated endocytosis [1,2,4]. In addition, with the encapsulated small size AuNRs, which had high energy absorbance at 808 nm NIR light, the liposomes could be readily heated up, thereby triggering the release of accompanying DOX. Therefore, the prepared systems could allow targeted delivery and on-demand drug liberation to possibly avoid adverse side effects. *In vitro* photothermal experiments showed that it took only 5 min for the liposomal solution to reach the hyperthermia temperature of more than 43 °C. Meanwhile, PBS solutions displayed only minimal temperature increase.

Through the fluorescent imaging, flow cytometry, and *in vitro* cytotoxicity tests, it was found that the targeting liposomes displayed the superior uptake by the 4T1 cells compared to the nontargeting liposomes, and showed higher cell cytotoxicity in NIR treatment group, thus it indicates that critically higher drug amount was released and entered the cell nuclei with the IC_{50} value of 1.90 ± 0.12 μg/mL, which was relatively close with that of the free DOX. The encouraging results were further validated using 4T1 tumor bearing BALB/C mice. The *in vivo* experiments showed that synergistic application of dual therapy with the FA targeting liposomes could effectively inhibit the tumor growth after the treatment. Meanwhile, the remaining monotherapies could only slow down the tumor development process.

Therefore, the present study proposed a potentially effective platform for the treatment of breast cancer. However, in order to make our system closer to clinical trials, our future study will focus on: (i) optimizing the composition parameters such as drug and gold nanoparticles encapsulation efficiency, drug loading, average size as well as the power and irradiation duration of the NIR system; and (ii) enhancing the targetability of the constructed systems; one possible approach can be the combination of different ligands, for instance, hyaluronic acid, FA, and/or antibodies into a single platform; another approach shall be the use additional magnetic elements in the liposomes and utilize external magnetic actuating system to guide the nanoparticles to the targeted area [6,37,38].

5. Conclusion

In summary, we have reported in this study the synthesis and evaluation of a novel drug delivery system for targeted drug delivery to FR overexpressing mouse origin breast cancer cells. The targeting liposomes, composed of DPPC, DSPE-PEG2000, DSPE-PEG2000-Folate, cholesterol, AuNRs, and DOX, were prepared and evaluated in-vitro and in-vivo. The average diameter of liposomes with an FA targeting ligand was smaller than 200 nm, enabling the delivery of DOX to cancer cells by both passive and active targeting pathways. The FA moiety grafted on the liposomal surfaces could significantly augment the cellular uptake of liposomes. Moreover, through the entrapment of AuNRs in the cores of the liposomes, DOX release could be enhanced when the liposomes were exposed to an 880-nm NIR laser. In addition, MTT results also suggested that NIR irradiation increased the cytotoxicity of the targeting liposomes. Finally, the results were further confirmed by *in vivo* test on 4T1 tumor-bearing mice, which showed that the developed nanosystems could effectively regress the tumor development. It, therefore, appears that the use of FA ligand-conjugated liposomes with synergistic application of photothermal-chemotherapy may offer an effective strategy to tackle the FR overexpressing cancers.

Acknowledgements

This work was supported by the Bio & Medical Technology Development Program of the National Research Foundation (NRF) funded by the Korean government (MSIT)2016M3A9E9941514 and the Industrial Technology Innovation Program [10060059, Externally Actuatable Nanorobot System for Precise Targeting and Controlled Releasing of Drugs] funded by the Ministry of Trade, Industry and Energy (MOTIE, Korea). The authors thank Dr. Shaohui Zheng for helpful discussions and Mr. Viet Ha Le for his assistance in illustrating the figures.

Appendix A. Supplementary data

Supplementary material related to this article can be found, in the online version, at doi:https://doi.org/10.1016/j.colsurfb.2018.10.013.

References

[1] T.M. Allen, P.R. Cullis, Drug delivery systems: entering the mainstream, Science 303 (2004) 1818–1822.
[2] S. Wilhelm, A.J. Tavares, Q. Dai, S. Ohta, J. Audet, H.F. Dvorak, W.C.W. Chan, Analysis of nanoparticle delivery to tumours, Nat. Rev. Mater. 1 (2016) 16014.
[3] A. Wicki, D. Witzigmann, V. Balasubramanian, J. Huwyler, Nanomedicine in cancer therapy: challenges, opportunities, and clinical applications, J. Controlled Release 200 (2015) 138–157.
[4] M.S. Muthu, S.A. Kulkarni, A. Raju, S.S. Feng, Theranostic liposomes of TPGS coating for targeted co-delivery of docetaxel and quantum dots, Biomaterials 33 (2012) 3494–3501.
[5] J. You, P. Zhang, F. Hu, Y. Du, H. Yuan, J. Zhu, Z. Wang, J. Zhou, C. Li, Near-infrared light-sensitive liposomes for the enhanced photothermal tumor treatment by the combination with chemotherapy, Pharm. Res. 31 (2014) 554–565.
[6] V.D. Nguyen, J. Han, G. Go, J. Zhen, S. Zheng, V.H. Le, J.-O. Park, S. Park, Feasibility study of dual-targeting paclitaxel-loaded magnetic liposomes using electromagnetic actuation and macrophages, Sens. Actuators B: Chem. 240 (2017) 1226–1236.
[7] Z. Li, H. Huang, S. Tang, Y. Li, X.-F. Yu, H. Wang, P. Li, Z. Sun, H. Zhang, C. Liu, P.K. Chu, Small gold nanorods laden macrophages for enhanced tumor coverage in photothermal therapy, Biomaterials 74 (2016) 144–154.
[8] M.R.K. Ali, M.A. Rahman, Y. Wu, T. Han, X. Peng, M.A. Mackey, D. Wang, H.J. Shin, Z.G. Chen, H. Xiao, R. Wu, Y. Tang, D.M. Shin, M.A. El-Sayed, Efficacy, long-term toxicity, and mechanistic studies of gold nanorods photothermal therapy of cancer in xenograft mice, Proceedings of the National Academy of Sciences, (2017).
[9] A. Agarwal, M.A. Mackey, M.A. El-Sayed, R.V. Bellamkonda, Remote triggered release of doxorubicin in tumors by synergistic application of thermosensitive liposomes and Gold nanorods, ACS Nano 5 (2011) 4919–4926.
[10] W.I. Choi, J.-Y. Kim, C. Kang, C.C. Byeon, Y.H. Kim, G. Tae, Tumor regression in vivo by photothermal therapy based on gold-nanorod-loaded, functional nanocarriers, ACS Nano 5 (2011) 1995–2003.
[11] V.D. Nguyen, S. Zheng, J. Han, V.H. Le, J.-O. Park, S. Park, Nanohybrid magnetic liposome functionalized with hyaluronic acid for enhanced cellular uptake and near-infrared-triggered drug release, Colloids Surf. B. Biointerfaces 154 (2017) 104–114.
[12] J. You, R. Shao, X. Wei, S. Gupta, C. Li, Near-infrared light triggers release of paclitaxel from biodegradable microspheres: photothermal effect and enhanced antitumor activity, Small (Weinheim an der Bergstrasse, Germany) 6 (2010) 1022–1031.
[13] X. Wang, J. Zhang, Y. Wang, C. Wang, J. Xiao, Q. Zhang, Y. Cheng, Multi-responsive photothermal-chemotherapy with drug-loaded melanin-like nanoparticles for synergetic tumor ablation, Biomaterials 81 (2016) 114–124.
[14] J. Bai, Y. Liu, X. Jiang, Multifunctional PEG-GO/CuS nanocomposites for near-infrared chemo-photothermal therapy, Biomaterials 35 (2014) 5805–5813.
[15] K. Dong, Z. Liu, Z. Li, J. Ren, X. Qu, Hydrophobic anticancer drug delivery by a 980 nm laser-driven photothermal vehicle for efficient synergistic therapy of cancer cells in vivo, Adv. Mater. 25 (2013) 4452–4458.
[16] S. Sabharanjak, S. Mayor, Folate receptor endocytosis and trafficking, Adv. Drug Del. Rev. 56 (2004) 1099–1109.
[17] F. Tavassolian, G. Kamalinia, H. Rouhani, M. Amini, S.N. Ostad, M.R. Khoshayand, F. Atyabi, M.R. Tehrani, R. Dinarvand, Targeted poly (l-γ-glutamyl glutamine) nanoparticles of docetaxel against folate over-expressed breast cancer cells, Int. J. Pharm. 467 (2014) 123–138.
[18] M. Alibolandi, K. Abnous, F. Sadeghi, H. Hosseinkhani, M. Ramezani, F. Hadizadeh, Folate receptor-targeted multimodal polymersomes for delivery of quantum dots and doxorubicin to breast adenocarcinoma: in vitro and in vivo evaluation, Int. J. Pharm. 500 (2016) 162–178.
[19] M. Rezazadeh, J. Emami, F. Hasanzadeh, H. Sadeghi, M. Minaiyan, A. Mostafavi, M. Rostami, A. Lavasanifar, In vivo pharmacokinetics, biodistribution and antitumor effect of paclitaxel-loaded targeted chitosan-based polymeric micelle, Drug Deliv. 23 (2016) 1707–1717.
[20] H. Elnakat, M. Ratnam, Distribution, functionality and gene regulation of folate receptor isoforms: implications in targeted therapy, Adv. Drug Del. Rev. 56 (2004) 1067–1084.
[21] V. Dixit, J. Van den Bossche, D.M. Sherman, D.H. Thompson, R.P. Andres, Synthesis and grafting of thioctic Acid − PEG − Folate conjugates onto Au nanoparticles for selective targeting of folate receptor-positive tumor cells, Bioconj. Chem. 17 (2006) 603–609.
[22] M.R.K. Ali, B. Snyder, M.A. El-Sayed, Synthesis and optical properties of small Au nanorods using a seedless growth technique, Langmuir 28 (2012) 9807–9815.
[23] J.-H. Park, H.-J. Cho, H.Y. Yoon, I.-S. Yoon, S.-H. Ko, J.-S. Shim, J.-H. Cho, J.H. Park, K. Kim, I.C. Kwon, D.-D. Kim, Hyaluronic acid derivative-coated nanohybrid liposomes for cancer imaging and drug delivery, J. Controlled Release 174 (2014) 98–108.
[24] P. Pradhan, J. Giri, F. Rieken, C. Koch, O. Mykhaylyk, M. Döblinger, R. Banerjee, D. Bahadur, C. Plank, Targeted temperature sensitive magnetic liposomes for thermo-chemotherapy, J. Controlled Release 142 (2010) 108–121.
[25] Y. Liu, J. Sun, W. Cao, J. Yang, H. Lian, X. Li, Y. Sun, Y. Wang, S. Wang, Z. He, Dual targeting folate-conjugated hyaluronic acid polymeric micelles for paclitaxel delivery, Int. J. Pharm. 421 (2011) 160–169.
[26] M. Kamat, K. El-Boubbou, D.C. Zhu, T. Lansdell, X. Lu, W. Li, X. Huang, Hyaluronic acid immobilized magnetic nanoparticles for active targeting and imaging of macrophages, Bioconj. Chem. 21 (2010) 2128–2135.
[27] Q. Sun, Q. You, J. Wang, L. Liu, Y. Wang, Y. Song, Y. Cheng, S. Wang, F. Tan, N. Li, Theranostic nanoplatform: triple-modal imaging-guided synergistic cancer therapy based on liposome-conjugated mesoporous silica nanoparticles, ACS Appl. Mater. Interfaces 10 (2018) 1963–1975.
[28] C. Wang, H. Xu, C. Liang, Y. Liu, Z. Li, G. Yang, L. Cheng, Y. Li, Z. Liu, Iron oxide @ polypyrrole nanoparticles as a multifunctional drug carrier for remotely controlled cancer therapy with synergistic antitumor effect, ACS Nano 7 (2013) 6782–6795.
[29] W.-C. Huang, I.L. Lu, W.-H. Chiang, Y.-W. Lin, Y.-C. Tsai, H.-H. Chen, C.-W. Chang, C.-S. Chiang, H.-C. Chiu, Tumortropic adipose-derived stem cells carrying smart nanotherapeutics for targeted delivery and dual-modality therapy of orthotopic glioblastoma, J. Controlled Release 254 (2017) 119–130.
[30] X. Li, M. Takashima, E. Yuba, A. Harada, K. Kono, PEGylated PAMAM dendrimer–doxorubicin conjugate-hybridized gold nanorod for combined photothermal-chemotherapy, Biomaterials 35 (2014) 6576–6584.
[31] H. Li, J. Zhen, S. Cho, M.J. Jeon, V.D. Nguyen, J.-O. Park, S. Park, Folate receptor-targeted nir-sensitive polydopamine nanoparticles for chemo-photothermal cancer therapy, Nanotechnology 28 (2017) 425101.
[32] S.-M. Lee, H. Park, J.-W. Choi, Y.N. Park, C.-O. Yun, K.-H. Yoo, Multifunctional nanoparticles for targeted chemophotothermal treatment of cancer cells, Angew.

Chem. 123 (2011) 7723–7728.
[33] S.J. Park, S.H. Park, S. Cho, D.M. Kim, Y. Lee, S.Y. Ko, Y. Hong, H.E. Choy, J.J. Min, J.O. Park, S. Park, New paradigm for tumor theranostic methodology using bacteria-based microrobot, Sci. Rep. 3 (2013) 3394.
[34] S. Zheng, V.D. Nguyen, S.Y. Song, J. Han, J.-O. Park, Combined photothermal-chemotherapy of breast cancer by near infrared light responsive hyaluronic acid-decorated nanostructured lipid carriers, Nanotechnology 28 (2017) 435102.
[35] G.D. Bothun, A. Lelis, Y. Chen, K. Scully, L.E. Anderson, M.A. Stoner, Multicomponent folate-targeted magnetoliposomes: design, characterization, and cellular uptake, Nanomed. Nanotechnol. Biol. Med. 7 (2011) 797–805.
[36] M.R.K. Ali, S.R. Panikkanvalappil, M.A. El-Sayed, Enhancing the efficiency of Gold nanoparticles treatment of cancer by increasing their rate of endocytosis and cell accumulation using rifampicin, J. Am. Chem. Soc. 136 (2014) 4464–4467.
[37] D. Li, H. Choi, S. Cho, S. Jeong, Z. Jin, C. Lee, S.Y. Ko, J.-O. Park, S. Park, A hybrid actuated microrobot using an electromagnetic field and flagellated bacteria for tumor-targeting therapy, Biotechnol. Bioeng. 112 (2015) 1623–1631.
[38] J. Han, J. Zhen, V.D. Nguyen, G. Go, Y. Choi, S.Y. Ko, J.-O. Park, S. Park, Hybrid-actuating macrophage-based microrobots for active cancer therapy, Sci. Rep. 6 (2016) 28717.